Synthesis, Structural and Magnetic Characterization of a New Scheelite Related Compound: $Eu_2Mo_3O_{12}$

Khalid Boulahya,[a] Marina Parras,[a] and José M. González-Calbet*[a]

Keywords: Molybdate / X-ray diffraction / High resolution electron microscopy / Magnetic properties

Polycrystalline $Eu_2Mo_3O_{12}$ has been synthesized and characterized by X-ray and electron diffraction, high resolution electron microscopy and magnetic measurements. This oxide shows a complex scheelite superstructure whose essential feature is the existence of isolated Mo tetrahedra. Each Mo atom has four oxygen neighbors at distances ranging from 1.75 to 1.91 Å, whereas each Eu atom has eight oxygen neighbors at 2.43 Å. The temperature dependence of the inverse magnetic susceptibility shows that $Eu_2Mo_3O_{12}$ behaves as a Curie–Weiss paramagnet at high temperature (160–300 K), whereas in the range 100–20 K it shows Van Vleck paramagnetism.

Introduction

Rare earth molybdates constitute a large family of materials with interesting physical properties which depend on the crystal structure, rare earth element and molybdenum oxidation state. Initial interest was developed due to fluorescence properties.[1] Later on, new applications were reported for the molybdenum highest oxidation state (VI). Ferroelectric/ferroelastic properties have been described for $Gd_2Mo_3O_{12}$,[2] whereas La_2MoO_6[3] shows catalytic behavior and $La_2Mo_2O_9$[4] is a fast ionic conductor. More reduced molybdates present some interesting transport properties such as metal–insulator transitions, as is the case of $La_2Mo_2O_7$[5,6] which exhibits short Mo–Mo distances.

The chemical nature of the lanthanide element strongly influences its structural type. For instance, at least three polymorphs have been described for the $Ln_2Mo_3O_{12}$ complex. The $La_2Mo_3O_{12}$[7] structure is formed by a network of corner-sharing square-antiprismatic and tetrahedral sites, with La having eightfold and Mo slightly distorted tetrahedral oxygen coordination. The structure is related to the scheelite ($CaWO_4$) type,[8] from which it can be derived through vacancy ordering of one third of the Ca sites. Nearest-neighbor environments of the cations resemble those of the scheelite. $Gd_2Mo_3O_{12}$[2] presents two polymorphs with different symmetries; both structures contain a network of corner-sharing polyhedra in which Gd and Mo cations are coordinated by seven and four oxygen atoms, respectively. Tb and Mo stabilize the same oxygen environment in $Tb_2Mo_3O_{12}$.[9]

The europium-molybdenum systems are attractive as a result of their structural and compositional variation. Such variation arises from the ability of isolated MoO_4 tetrahedra and Mo_nO_m structural units to be incorporated, in an ordered manner, giving rise to the stabilization of phases with different Eu/Mo ratios. For instance, the crystal structure of $Eu_6Mo_{12}O_{45}$[10] comprises four MoO_4 tetrahedra, and Mo_2O_8 and $Mo_{12}O_{11}$ structural units which, connected by sharing corners, form polymeric $[Mo_4O_{17}]$ chains. $Eu_6Mo_{10}O_{39}$[11] and $Eu_2Mo_5O_{18}$[12] are formed by MoO_4 and Mo_2O_7 units, which are three-dimensionally arranged. $Eu_4Mo_7O_{27}$[11] is a layered compound consisting of MoO_4 and Mo_3O_{11} units, while $EuMoO_4$[13] adopts the scheelite structural type where isolated MoO_4 tetrahedra constitute the three-dimensional structure. Finally, the crystal structure of $Eu_6Mo_{10}O_{39}$[11] is characterized by bioctahedral Mo_{10} clusters forming extended chains.

In this work, we report the synthetic conditions and characterization, by means of X-ray Rietveld refinement, electron diffraction (ED), high resolution electron microscopy (HREM), electrical resistivity and magnetic susceptibility, of a new europium molybdate with the composition $Eu_2Mo_3O_{12}$. The structural relationship between this phase and the scheelite structural type is reported.

Results and Discussion

The cationic composition, as analyzed by energy-dispersive X-ray spectroscopy, is in agreement with the nominal composition, $Eu_2Mo_3O_{12}$. The corresponding X-ray powder diffraction pattern (Figure 1) can be fully indexed on the basis of a monoclinic unit cell with space group, *C*2/*c*, and lattice parameters $a = 7.5613(3)$ Å, $b = 11.4685(5)$ Å, $c = 11.5055(5)$ Å and $\beta = 109.309(3)°$, no extra reflections being detected.

---

[a] Departamento de Química Inorgánica, Facultad de Químicas, Universidad Complutense,
28040 Madrid, Spain
Fax: +34-91-394-43-52
E-mail: jgcalbet@quim.ucm.es

DOI: 10.1002/ejic.200400662

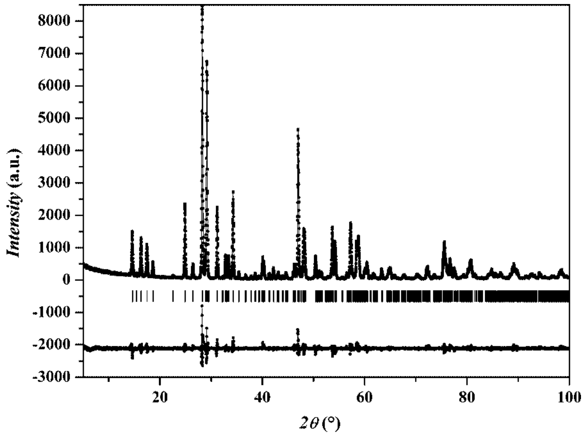

Figure 1. Experimental, calculated and difference X-ray diffraction patterns for $Eu_2Mo_3O_{12}$

The $Eu_2Mo_3O_{12}$ structure has been initially determined by ED and HREM (Figure 2). The HREM micrograph along the [100] zone axis (Figure 2b) shows an apparently well ordered material with d-spacings 5.7 and 3.6 Å, corresponding to d_{020} and d_{003}, respectively. Following the *b* axis, a layer of bright dots alternate with brighter ones in an ordered manner. This contrast can be associated with rows of tetrahedrally coordinated Mo atoms arranged at different heights along the *a* axis. These structural features are those presented by $Eu_2W_3O_{12}$[14] which can be described as a three-dimensional distribution of WO_4 tetrahedra linked by EuO_8 units. Therefore, from the $Eu_2W_3O_{12}$ atomic coordinates, an image calculation was performed in the *C*2/*c* space group. The simulated image (shown in the inset) compare well with the experimental one at Δt = 6 nm and Δf = –70 nm.

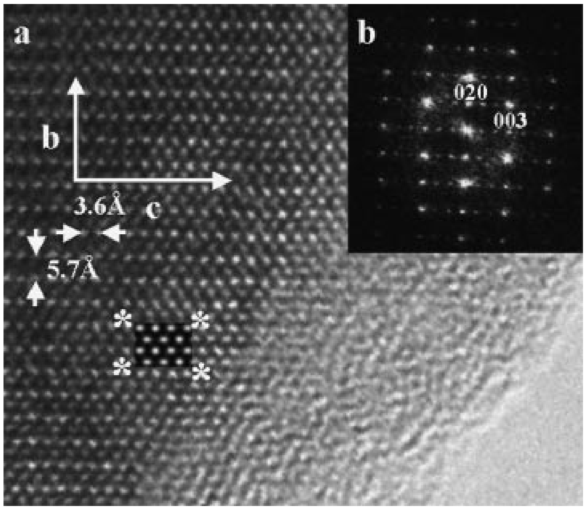

Figure 2. (a) HRTEM image of $Eu_2Mo_3O_{12}$ along [100], (b) corresponding FT. Simulated image is shown in the inset

On the basis of these results, an X-ray profile refinement was performed. The structure was solved in the ***C*2/*c*** space group taking the $Eu_2W_3O_{12}$ crystallographic data as the starting point. Peak shapes were described by pseudo-Voigt functions. Figure 1 shows the graphic results of the fitting of the experimental X-ray diffraction pattern and the difference between observed and calculated data. The refinement was stable and it was possible to refine the positions of oxygen atoms, provided a temperature factor for each type of atom was used. The structural model is depicted in Figure 3. The final structural parameters are collected in Table 1, whereas Table 2 shows some selected inter-atomic distances. The structure refinement confirms isotypism with $Eu_2W_3O_{12}$.[14] The crystal structure of the $Eu_2Mo_3O_{12}$ is formed by isolated $Mo(1)O_4$ tetrahedra and $Mo_2(2)O_8$ groups constituted by very irregular $Mo(2)O_5$ trigonal bipyramids. Mo1 forms a MoO_4 tetrahedron with M-O average distances of 1.78 or 1.83 Å. The Mo_2O_8 group comprises of two $Mo(2)O_5$ trigonal bipyramids sharing one edge. They are formed by three oxygen neighbors at distances of 1.79, 1.76, and 1.75 Å, a fourth one at 1.91 Å, and a fifth at 2.4 Å. Figure 4 shows a view of the Mo_2O_8 group. Such a dimeric group is also present in isostructural $Eu_2W_3O_{12}$ but, in this case, the distance to the fifth neighbor is smaller, close to 2.19 Å. However, a similar

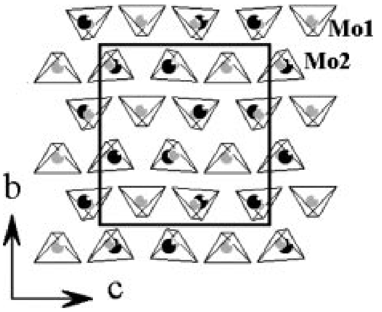

Figure 3. Structural model along *a*-axis of $Eu_2Mo_3O_{12}$. Black dots represent Eu atoms whereas grey dots correspond to Mo atoms

Table 1. Final structural parameters of $Eu_2Mo_3O_{12}$

Atom	*x*/*a*	*y*/*b*	*z*/*c*	*B* (Å^2)	Occ.
Eu1	0.3325(6)	0.3771(3)	0.4089(2)	1.106(85)	1
Mo1	0	0.1293(5)	1/4	1.75(11)	1
Mo2	0.1491(8)	0.3885(3)	0.0594(2)	1.75(11)	1
O1	0.173(3)	0.046(1)	0.214(2)	1.36(21)	1
O2	0.136(3)	0.211(2)	0.387(2)	1.36(21)	1
O3	0.250(3)	0.313(2)	0.198(2)	1.36(21)	1
O4	0.346(3)	0.461(1)	0.039(2)	1.36(21)	1
O5	0.033(3)	0.475(2)	0.394(2)	1.36(21)	1
O6	0.449(3)	0.208(2)	0.064(2)	1.36(21)	1

S.G. C 2/c (15), a = 7.5613(3) Å, b = 11.4685(5) Å, c = 11.5055(5) Å,
β = 109.309(3)° V = 941.598(63) Å^3,
R_B = 0.041, R_{exp} = 0.064, R_{wp} = 0.113, χ^2 = 3.12.

Table 2. Selected inter-atomic distances (Å) in $Eu_2Mo_3O_{12}$

Eu1–O1: 2.39 (2)	Mo1–O1: 1.78 (2)
Eu1–O2: 2.38 (2)	Mo1–O2: 1.83 (2)
Eu1–O2: 2.49 (2)	Mo2–O3: 1.75 (2)
Eu1–O3: 2.41 (2)	Mo2–O4: 1.79 (2)
Eu1–O4: 2.49 (2)	Mo2–O5: 1.91 (2)
Eu1–O4: 2.37 (2)	Mo2–O6: 1.76 (2)
Eu1–O5: 2.48 (3)	Mo2–O5: 2.40 (2)[a]
Eu1–O6: 2.49 (2)	Mo2–Mo2: 3.38 (2)

value (2.39 Å) is observed in the related oxide $Eu_4Mo_7O_{27}$.[11] The Eu atom has eight oxygen neighbors at an average distance of 2.43 Å with a distorted square-antiprismatic coordination as observed in related europium oxides.[11]

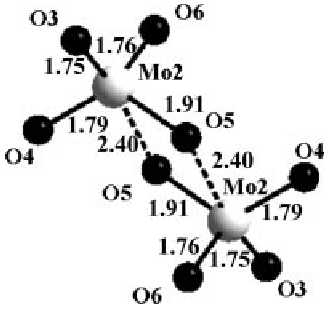

Figure 4. Structural details of the Mo_2O_8 group

The $EuMoO_4$,[13] scheelite related structure is depicted in Figure 5a. The analogy with $Eu_2Mo_3O_{12}$ can be clearly seen by comparing Figures 5a and b. Both structures are formed by similar $[MoO_4]$ units of isolated tetrahedra. The essential structural difference is related to the europium atoms planes. In the scheelite $EuMoO_4$ structure, the three crystallographic Eu planes, indicated by solid lines in Figure 5a, are fully occupied and equidistant along the [120] direction. The ordered elimination of one of every three Eu planes in $EuMoO_4$, leads to the $Eu_2Mo_3O_{12}$ structure (Figure 5b). This Eu elimination process has less influence on the Eu coordination than in the Mo one. Whereas in the scheelite structure Mo only adopts tetrahedral coordination, in the $Eu_2Mo_3O_{12}$ oxide, Mo is also trigonal bipyramidally coordinated.

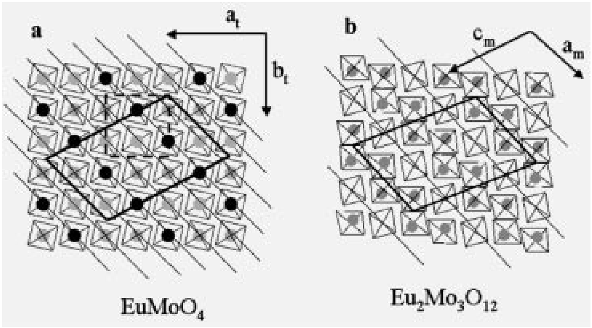

Figure 5. Schematic representation of the structural relationship between (a) $EuMoO_4$ and (b) $Eu_2Mo_3O_{12}$. Both structures are projected along the *c* axis of the scheelite cell, which is outlined by broken lines. Black dots represent the Eu atoms, which are eliminated in $Eu_2Mo_3O_{12}$. The steps involving the $EuMoO_4$ to $Eu_2Mo_3O_{12}$ transformation are shown

From the crystallographic point of view, monoclinic ($C2/c$) $Eu_2Mo_3O_{12}$ can be considered as a superstructure of tetragonal ($I4_1/a$) $EuMoO_4$ as depicted in Figure 5a. The monoclinic cell parameters a_m, b_m, and c_m can be related to the tetragonal ones a_t and c_t by means of the expression: $a_m \approx a_t\sqrt{2}$, $b_m \approx c_t$ and $c_m \approx a_t\sqrt{5}$. Furthermore, the symmetry $C2/c$ is a subgroup of $I4_1/a$.

On the other hand, different physical properties have also been explored. First, from an electrical point of view, $Eu_2Mo_3O_{12}$ behaves as an insulator at room temperature.

The temperature dependence of the molar susceptibility is shown in Figure 6. The curve shape resembles that reported by Holsa et al.[15] but χ is smaller by 14–30% than their data at all the temperatures measured. The χ^{-1} value follows the Curie–Weiss law down to about 160 K and then is constant for the lower temperature range between 100 and 20 K. Finally, below 20 K, a sharp decrease in the inverse susceptibility is observed. This behavior can be qualitatively explained by the exceptional ^7F_J (J = 0–6) ground term energy level Scheme of the Eu^{3+} ion.[16,17] The $^7F_0$–$^7F_1$ energy gap is large enough to induce a *plateau* in the inverse paramagnetic susceptibility curve due to the constant temperature independent paramagnetism, since practically only the ground level $^7F_0$ is populated. The $^7F_0$ ground level is non-magnetic and gives no contribution to the $Eu_2Mo_3O_{12}$ susceptibility at low temperatures. At the higher temperature range, the population of the closely spaced higher ^7F_J (J = 1–6) levels leads to the normal Curie–Weiss paramagnetism. It can be concluded that for Eu^{3+}, the crystal field plays a significant role in the susceptibility. Below 15 K, a sharp decrease in the inverse susceptibility is observed. This has been already been observed with other Eu compounds, as in the oxychloride EuOX (X = Br, Cl),[15,16] and attributedto the presence of a slight amount of Eu^{2+} impurity, since Eu^{2+} with the $^4f_7$ electron configuration has high paramagnetic susceptibility. In order to understand this phenomenon, a study on partially reduced Eu^{3+} samples is in progress.

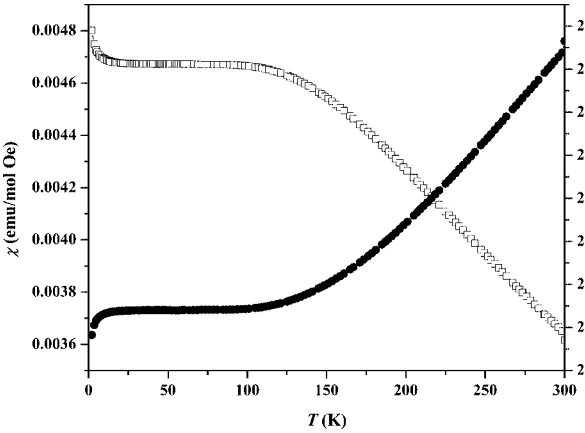

Figure 6. Temperature evolution of the magnetic susceptibility χ (squares) and χ^{-1} (black dots) of $Eu_2Mo_3O_{12}$

Experimental Section

Polycrystalline $Eu_2Mo_3O_{12}$ was synthesised by heating stoichiometric amounts of Eu_2O_3 (Aldrich; 99.98%) and MoO_2 (Aldrich; 99+%) in air at 900 °C for 4 days and then quenched to room temperature.

Powder X-ray diffraction patterns were collected with CuKα radiation at room temperature on a PHILIPS X'PERT diffractometer equipped with a graphite monochromator. Diffraction data were analyzed by the Rietveld method[18] using the Fullprof program.[19]

The sample was characterized by ED and HREM using a PHILIPS CM200 FEG electron microscope, fitted with a double tilting goniometer stage (±40°, ±24°). Local composition was analyzed with an EDAX DX-4 analyzer system attached to the above microscope. Simulated HREM images were calculated by the multislice method using the MacTempas software package. Magnetic properties were measured with a SQUID magnetometer, over the temperature range 2 to 300 K, and magnetic fields up to 5 T.

Acknowledgments

Financial support through research project MAT2001-1440 is acknowledged. K. B. thanks the MCYT (Spain) for financial support under the "Ramón y Cajal" Program.

---

[1] R. MacDonald, M. Vogel, J. Brookman, *IBM J. Res. Dev.* **1962**, *6*, 363.

[2] E. T. Keve, S. C. Abrahams, J. L. Berstein, *J. Chem. Phys.* **1971**, *54*, 3185–3194; W. Jeitschko, *Acta Crystallogr., Sect. B* **1972**, *28*, 60–76.

[3] J. S. Xue, M. R. Antonio, L. Soderholm, *Chem. Mater.* **1995**, *7*, 333–340.

[4] P. Lacorre, F. Goutenoire, R. Retoux, Y. Laligant, *Nature* **2000**, *404*, 856–858.

[5] A. Moini, M. A. Subramanian, A. Clearfield, F. J. DiSalvo, W. H. McCaroll, *J. Solid State Chem.* **1987**, *66*, 136–143.

[6] T. Mingliang, M. Zhiqiang, Z. Yuheng, *J. Phys.*: *Condens. Matter* **1996**, *8*, 3413–3418.

[7] W. Jeitschko, *Acta Crystallogr. Sect. B* **1973**, *29*, 2074–2078.

[8] L. G. Sillen, A. Nylander, *Ark. Kem.* **1943**, *17A*, 1.

[9] C. Svensson, S. C. Abrahams, J. L. Berstein, *J. Chem. Phys.* **1979**, *71*, 5191–5195.

[10] H. Naruke, T. Yamase, *Inorg. Chem.* **2002**, *41*, 6514–6520.

[11] H. Naruke, T. Yamase, *J. Solid State Chem.* **2001**, *161*, 85–92.

[12] P. Gougeon, P. Gall, J. F. Halet, R. Gautier, *Acta Crystallogr., Sect. B* **2003**, *59*, 472–79.

[13] G. J. McCarthy, *Mater. Res. Bull.* **1971**, *6*, 31–39.

[14] H. D. Templeton, A. Zalkin, *Acta Crystallogr.* **1963**, *16*, 762–766.

[15] J. Holsa, M. Lastusaari, J. Niittykoski, R. Saez Puche, *Phys. Chem. Chem. Phys.* **2002**, *4*, 3091–3097.

[16] T. Aitasalo, J. Holsa, M. Lastusaari, J. Legendziewicz, L. Lehto, J. Linden, M. Marysko, *J. Alloys Compd.*, in press.

[17] S. Ebisu, T. Sogabe, H. Morita, S. Nagata, *J. Magn. Magn. Mater.* **1998**, *177*, 1073–1074.

[18] H. V. Rietveld, *J. Appl. Crystallogr.* **1969**, *2*, 65–71.

[19] J. Rodríguez-Carvajal, *J. Physica* **1993**, *B192*, 55–69.

Received: July 29, 2004